Chapter 7

Hall effects on unsteady MHD reactive flow through a porous channel with convective heating under Arrhenius reaction rate*

7.1 Introduction

Magnetohydrodynamics (MHD) is concerned with the mutual interaction of a conducting fluid flow and magnetic field. The fluids being investigated are electrically conducting and nonmagnetic, which limits them to liquid metals, hot ionized gases (plasmas) and strong electrolytes. Fluid flows under the influence of an applied magnetic field occur in certain engineering processes like glass manufacturing, crude oil refinement, paper production, polymer technology, petroleum industries, geothermal energy extraction and boundary-layer control in the field of aerodynamics and blood flow. In recent years, hydromagnetic flow and heat transfer in it have received considerable attention due to their various applications in science, engineering and industry. Several authors have studied the magnetohydrodynamic flow and heat transfer under various physical situations [374-392].

When a strong magnetic field is applied, the influence of electromagnetic force is noticeable and this field induces many complex phenomenons in an electrically conduct-

*Published in **Journal of Engineering Physics and Thermophysics, 90(5)(2017), pp.1240-1253.***

ing flow regime including the Hall currents, Joule heating etc., as stated by Cramer and Pai [12]. In fact, in an ionized gas in a strong magnetic field when the density is low, the Hall current is induced perpendicularly to both electric and magnetic fields. It has significant effect on the current density and hence on the electromagnetic force. Sutton and Sherman [355] have investigated a hydromagnetic flow of a viscous ionized gas between two parallel plates taking the Hall effects into account. It is the first significant study to include Hall effects where it is indicated that a fluid flow in a parallel plate channel becomes secondary in nature. The Hall currents have a significant effect on the magnitude and direction of the current density and consequently on the magnetic force. A theoretical study of unsteady magnetohydrodynamic viscous HartmannCouette laminar flow and heat transfer in a Darcian channel with the Hall current, ion slip as well as viscous and Joule heating effects have been explained by Bég et al. [238] under a constant pressure gradient. Ghosh et al. [250] have studied the Hall effects on an MHD flow in a rotating system. Ghosh et al. [253] have obtained a closed form solutions for the transient hydromagnetic flow in a rotating channel with inclined applied magnetic field under the influence of a forced oscillation. A numerical study on MHD generalized Couette flow and heat transfer with variable viscosity and electrical conductivity have been performed by Makinde and Onyejekwe [243]. Makinde and Chinyoka [202] have studied an unsteady hydromagnetic generalized Couette flow and heat transfer characteristics of a reactive variable viscosity incompressible electrically conducting third grade fluid in a channel with asymmetric convective cooling at the walls in the presence of uniform transverse magnetic field. Ghara et al. [43] have examined the unsteady MHD Couette flow of an incompressible viscous electrically conducting fluid between two infinite nonconducting horizontal porous plates under the boundary layer approximations considering both Hall currents and ion-slip. Abd El-Meged et al. [393] have obtained an analytical solution for a transient Hartmann flow with the Hall current and ion slip.

In almost all of the above mentioned studies, constant fluid properties are assumed. However, experiments indicate that this can hold only if the temperature does not change rapidly or impulsively. Hence, more accurate prediction of flow and heat transfer can be obtained only by considering variations of the fluid and electromagnetic properties, especially the temperature variations of the fluid viscosity, thermal conductivity and the electrical conductivity. Generally speaking, most lubricants used in both engineering and industrial processes are reactive, e.g. hydrocarbon oils, polyglycols, synthetic esters, polyphenylethers etc., and their efficiency depends largely on the temperature variation. Thus, it is important to determine the heat transfer conditions and

thermal loading properties of viscous reactive fluids to estimate their effectiveness as lubricants. The second law analysis of a Couette flow of a reactive fluid with variable viscosity and the Arrhenius kinetics has been carried out by Kobo and Makinde [270]. Das et al. [394] have considered the Hall effects on MHD Couette flow in a rotating system. Chinyoka and Makinde [395] have studied a transient generalized Couette flow of a reactive variable viscosity third-grade liquid with asymmetric convective cooling. Makinde and Eegunjobi [244] have analyzed the inherent irreversibility in an MHD generalized Couette flow of variable viscosity. Theuri and Makinde [396] have presented the thermodynamic analysis of an MHD unsteady generalized Couette flow of a viscous fluid with variable viscosity. The steady generalized axial Couette flow of power law reactive fluids between concentric cylindrical pipes has been presented by Makinde [273]. Makinde and Franks [272] have investigated the effect of magnetic field on a reactive unsteady generalized Couette flow with temperature dependent viscosity and thermal conductivity. Das et al. [397] have considered transient hydromagnetic reactive Couette flow and heat transfer in a rotating frame of reference. Veera Krishna and Swarnalathamma [398] have demonstrated the Hall effects on an unsteady MHD reactive flow of second grade fluid through porous medium in a rotating parallel plate channel.

This chapter is devoted to investigate the effects of the Hall currents on an unsteady hydromagnetic flow of a reactive, viscous, incompressible, electrically conducting fluid between infinite horizontal parallel plates. The governing momentum equations are solved analytically by the Laplace transform technique. It is assumed that a conducting incompressible fluid is subjected to an exothermic reaction with the Arrhenius kinetics and neglecting the consumption of the material.

7.2 Mathematical Formulation

Consider an unsteady MHD flow of a viscous incompressible electrically conducting fluid between two infinite horizontal parallel plates. Let h be the distance between these plates and h be small in comparison with the characteristic length of the plates. The upper plate moves with a velocity $\mathrm{U}(t)$ which is a known function of time t in its own plane in the x-direction, where the x-axis is placed on the lower stationary plate. The y-axis is normal to the x-axis and the z-axis is normal to the xy-plane (see Fig.7.1). It is assumed that the flow is fully developed. Further, there is no applied pressure gradient as the flow is due to the motion of the upper plate. A uniform transverse magnetic field of strength B_0 is applied perpendicular to the plates with uniform

suction/injection. Initially, at time $t \leq 0$, the plates and fluid are assumed to be at the same temperature T_0 and stationary. At time $t > 0$, the plate at $y = h$ starts to move in its own plane with the velocity U(t), whereas the plate at $y = 0$ is stationary. The plates are maintained at a constant temperature T_0. Since the plates are infinitely long along the x- and z-directions, all physical quantities are functions of y and t only. The equation of continuity then yields $v = -v_0$ everywhere in the fluid.

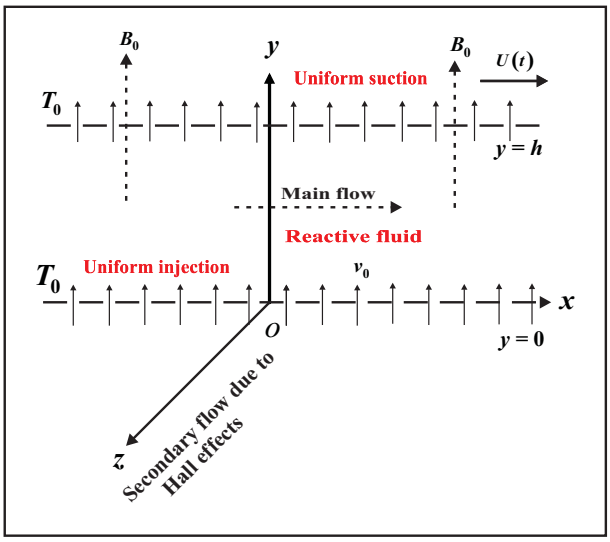

Fig.7.1 : *Geometry of the problem*

The generalized Ohm's law with the Hall currents taken into account is [7]

$$\vec{j} + \frac{\omega_e \tau_e}{B_0}\left(\vec{j} \times \vec{B}\right) = \sigma\left(\vec{E} + \vec{q} \times \vec{B}\right), \tag{7.1}$$

where $\vec{q}$, $\vec{B}$, $\vec{E}$, $\vec{j}$, σ, ω_e and τ_e are respectively the velocity vector, the magnetic field vector, the electric field vector, the current density vector, electrical conductivity, cyclotron frequency and electron collision time. Here the ion slip and thermoelectric effects as well as the electron pressure gradient are neglected. The quantity in the parenthesis on the right-hand side is the electric field in a rotating frame. The first term on the left-hand side is the electron drag on the ions and the second term is the Hall term according to the idea that electrons and ions can decouple and moves separately. It is assumed that the magnetic Reynolds number is very small so that the induced magnetic field can be neglected [7]. This assumption is justified since the magnetic Reynolds number is generally very small for metallic and partially ionized fluids.

The magnetic Reynolds number is the magnetic analogue of the Reynolds number and describes the interaction of fluids with a magnetic field. At high values of the magnetic Reynolds number, the magnetic field moves with the flow and this constitutes the frozen-in scenario which is important for the induction problems. When the magnetic Reynolds number is much less than unity, the magnetic field is not distorted by the flow field. When this number is small, the induced magnetic field is negligible in comparison to the applied one. The magnetic Prandtl number $\mathrm{P_m}$ is the ratio of the magnetic Reynolds number to the ordinary one, i.e. the ratio of the kinematic viscosity to the magnetic diffusivity. The number $\mathrm{P_m}$ is generally less, but not greatly less, than unity in induced magnetohydrodynamic flows. It measures the relative magnitude of the hydrodynamic and magnetic boundary layer thicknesses. For liquid metals, $\mathrm{P_m} \sim 10^{-9}$ to 10^{-5}, i.e. it is extremely low, since the magnetic diffusivity of such fluids is very high. The value $\mathrm{P_m} = 0.72$ corresponds to ionized hydrogen. In astrophysical flows, at the base of the solar convection zone, $\mathrm{P_m}$ attains the value 10^{-2} (Ghosh et at.[253]).

The solenoidal relation $\nabla \cdot \vec{B} = 0$ gives $B_y = \text{constant} = B_0$ everywhere in the flow, where $\vec{B} \equiv (0, B_y, 0)$. The expression for the conservation of electric current $\nabla \cdot \vec{j} = 0$ yields $j_z = \text{constant}$, where $\vec{j} \equiv (j_x,\ j_y,\ j_z)$. This constant is zero since $j_y = 0$ at the plates that are electrically non-conducting. Hence, $j_y = 0$ everywhere in the flow. In view of the above assumptions, equation (7.1) yields

$$j_x - m j_z = \sigma(E_x - w\, B_0), \tag{7.2}$$

$$j_z + m j_x = \sigma(E_z + u\, B_0), \tag{7.3}$$

where $m = \omega_e\, \tau_e$ is the Hall parameter which can take positive or negative values. In general, for an electrically conducting fluid, the Hall currents affect the flow in the presence of a strong magnetic field. The effect of the Hall currents gives rise to a force in the z-direction, which induces a cross flow in that direction. To simplify the problem, it is assumed that there are no variations in the flow quantities in the z-direction. This assumption is justified as the plate is of infinite extent in the z-direction.

Since the induced magnetic field is neglected, Maxwell's equation $\nabla \times \vec{E} = -\frac{\partial \vec{B}}{\partial t}$ becomes $\nabla \times \vec{E} = 0$ which yields $\frac{\partial E_x}{\partial y} = 0$ and $\frac{\partial E_z}{\partial y} = 0$. This implies that $E_x = \text{constant}$ and $E_z = \text{constant}$ everywhere in the flow.

Obtaining j_x and j_z from equations (7.2) and (7.3), we have

$$j_x = \frac{\sigma}{1+m^2}\left[B_0\,(mu - w) + (E_x + mE_z)\right], \tag{7.4}$$

$$j_z = \frac{\sigma}{1+m^2}\left[B_0\,(u + mw) + (E_z - mE_x)\right]. \tag{7.5}$$

Assuming that $j_x = 0$ and $j_z = 0$ at the plate $y = h$, since the channel plates are electrically non-conducting and using the boundary condition at this plate, we have

$$j_x = \frac{\sigma B_0}{1+m^2}\left[m(u-\mathrm{U}) - w\right], \tag{7.6}$$

$$j_z = \frac{\sigma B_0}{1+m^2}\left[(u-\mathrm{U}) + mw\right]. \tag{7.7}$$

Using equations (7.6) and (7.7), we write the Navier-Stokes equations of motion as

$$\frac{\partial u}{\partial t} - v_0\frac{\partial u}{\partial y} = -\frac{1}{\rho}\frac{\partial p}{\partial x} + \nu\frac{\partial^2 u}{\partial y^2} - \frac{\sigma B_0^2}{\rho(1+m^2)}\left[(u-\mathrm{U}) + mw\right], \tag{7.8}$$

$$\frac{\partial w}{\partial t} - v_0\frac{\partial w}{\partial y} = -\frac{1}{\rho}\frac{\partial p}{\partial z} + \nu\frac{\partial^2 w}{\partial y^2} + \frac{\sigma B_0^2}{\rho(1+m^2)}\left[m(u-\mathrm{U}) - w\right], \tag{7.9}$$

where u and w are the fluid velocity components along the x- and z-directions respectively, ρ the fluid density, ν the kinematic viscosity and p the fluid pressure. Equations (7.8) and (7.9) describe a hydromagnetic flow of any conducting medium between infinite horizontal parallel plates due to the motion of the upper plate.

The initial and boundary conditions are

$$\begin{aligned} &t \le 0: \quad u = w = 0 \ \text{ for } \ 0 \le y \le h, \\ &t > 0: \quad u = w = 0 \ \text{ at } \ y = 0 \ \text{ and } \ u = \mathrm{U}(t), \ \ w = 0 \ \text{ at } \ y = h. \end{aligned} \tag{7.10}$$

After the use of the boundary condition at $y = h$, we have

$$\frac{\partial \mathrm{U}}{\partial t} = -\frac{1}{\rho}\frac{\partial p}{\partial x}, \ \ 0 = -\frac{1}{\rho}\frac{\partial p}{\partial z} \tag{7.11}$$

On the use of equation (7.11), equations (7.8) and (7.9) become

$$\frac{\partial u}{\partial t} - v_0\frac{\partial u}{\partial y} = \frac{\partial \mathrm{U}}{\partial t} + \nu\frac{\partial^2 u}{\partial y^2} - \frac{\sigma B_0^2}{\rho(1+m^2)}\left[(u-\mathrm{U}) + mw\right], \tag{7.12}$$

$$\frac{\partial w}{\partial t} - v_0\frac{\partial w}{\partial y} = \nu\frac{\partial^2 w}{\partial y^2} + \frac{\sigma B_0^2}{\rho(1+m^2)}\left[m\,(u-\mathrm{U}) - w\right]. \tag{7.13}$$

Introducing the non-dimensional variables

$$\eta = \frac{y}{h}, \ \ (u_1, w_1) = \frac{(u,w)}{u_0}, \ \ \tau = \frac{\nu t}{h^2}, \ \ \mathrm{U}(t) = u_0 f(\tau) \tag{7.14}$$

equations (7.12) and (7.13) become

$$\frac{\partial u_1}{\partial \tau} - \mathrm{Re}\frac{\partial u_1}{\partial \eta} = \frac{\partial f}{\partial \tau} + \frac{\partial^2 u_1}{\partial \eta^2} - \frac{M^2}{1+m^2}\left[u_1 - f(\tau) + mw_1\right], \tag{7.15}$$

$$\frac{\partial w_1}{\partial \tau} - \mathrm{Re}\frac{\partial w_1}{\partial \eta} = \frac{\partial^2 w_1}{\partial \eta^2} + \frac{M^2}{1+m^2}\left[m\left\{u_1 - f(\tau)\right\} - w_1\right], \tag{7.16}$$

where $M^2 = \frac{\sigma B_0^2 h^2}{\rho\nu}$ is the squared-Hartmann number representing the ratio of the electromagnetic (Lorentz) force to the viscous force, $\mathrm{Re} = \frac{v_0 h}{\nu}$ the suction/injection Reynolds number and u_0 being a constant.

The initial and boundary conditions (7.10) become

$$\begin{aligned} &\tau \le 0: \;\; u_1 = w_1 = 0 \;\text{ for }\; 0 \le \eta \le 1, \\ &\tau > 0: \;\; u_1 = w_1 = 0 \;\text{ at }\; \eta = 0 \;\text{ and }\; u_1 = f(\tau), \;\; w_1 = 0 \;\text{ at }\; \eta = 1. \end{aligned} \tag{7.17}$$

Combining equations (7.15) and (7.16), we get

$$\frac{\partial q}{\partial \tau} - \mathrm{Re}\frac{\partial q}{\partial \eta} \;\; = \;\; \frac{\partial f}{\partial \tau} + \frac{\partial^2 q}{\partial \eta^2} - \frac{M^2(1 - i\,m)}{1 + m^2}\left[q - f(\tau)\right], \tag{7.18}$$

where $q = u_1 + i\,w_1$ and $i = \sqrt{-1}$.

The initial and boundary conditions for $q(\eta, \tau)$ are

$$\begin{aligned} &\tau \le 0: \;\; q = 0 \;\text{ for }\; 0 \le \eta \le 1, \\ &\tau > 0: \;\; q = 0 \;\text{ at }\; \eta = 0 \;\text{ and }\; q = f \;\text{ at }\; \eta = 1. \end{aligned} \tag{7.19}$$

Performing the Laplace transformation, from equation (7.18), we obtain

$$\frac{d^2\bar{q}}{d\eta^2} + \mathrm{Re}\frac{d\bar{q}}{d\eta} - (s + a)\bar{q} = -(a + s)\bar{f}(s), \tag{7.20}$$

where

$$\bar{q}(\eta, s) = \int_0^\infty q(\eta, \tau)\, e^{-s\tau}\, d\tau, \;\; a = \frac{M^2\,(1 - i\,m)}{(1 + m^2)}. \tag{7.21}$$

The boundary conditions for $\bar{q}(\eta, s)$ are

$$\bar{q}(0, s) = 0 \;\text{ and }\; \bar{q}(1, s) = \bar{f}(s), \tag{7.22}$$

where $\bar{f}(s)$ is the Laplace transform of $f(\tau)$.

The solution of equation (7.20) subject to the boundary conditions (7.22) is given by

$$\bar{q}(\eta, s) \;\; = \;\; \bar{f}(s)\left[1 - \frac{e^{-\frac{Re}{2}\eta}\sinh\sqrt{a + s + \frac{\mathrm{Re}^2}{4}}\;(1 - \eta)}{\sinh\sqrt{a + s + \frac{\mathrm{Re}^2}{4}}}\right]. \tag{7.23}$$

7.2.1 When the upper plate is set into impulsive motion

For impulsive motion $f(\tau) = 1$, i.e. $\bar{f}(s) = \frac{1}{s}$. Then the inverse Laplace transform of the equation (7.23) gives the velocity field as

$$\begin{aligned} q(\eta,\tau) &= 1 - e^{-\frac{Re}{2}\eta}\left[\frac{\sinh(\alpha + i\ \beta)\ \ (1-\eta)}{\sinh(\alpha + i\ \beta)}\right. \\ &- \left. 2\ \sum_{n=1}^{\infty} \frac{e^{s_1\tau}}{s_1} \cdot n\pi\ \sin n\pi\eta\right], \end{aligned} \tag{7.24}$$

where

$$\begin{aligned} s_1 &= -\left(a + n^2\pi^2 + \tfrac{\mathrm{Re}^2}{4}\right), \\ \alpha,\beta &= \tfrac{1}{\sqrt{2}}\left[\left\{\left(\tfrac{M^2}{1+m^2} + \tfrac{\mathrm{Re}^2}{4}\right)^2 + \left(\tfrac{mM^2}{1+m^2}\right)^2\right\}^{\frac{1}{2}} \pm \left(\tfrac{M^2}{1+m^2} + \tfrac{\mathrm{Re}^2}{4}\right)\right]^{\frac{1}{2}}. \end{aligned} \tag{7.25}$$

Equation (7.24) represents the general solution for the unsteady, impulsively started, hydromagnetic flow through a channel with the magnetic lines of force fixed relative to the fluid. The solution (7.24) exists for both injection at the lower plate and suction at the upper moving plate. On separating equation (7.24) into real and imaginary parts, one can easily obtain the velocity components u_1 and w_1. In the absence of the Hall currents ($m = 0$), the present problem reduces to the problem studied by Makinde and Franks [272].

7.2.2 When the upper plate starts to move with uniform acceleration

For accelerated motion $f(\tau) = \tau$, i.e. $\bar{f}(s) = \frac{1}{s^2}$. The inverse Laplace transform of equation (7.23) yields the velocity field as

$$\begin{aligned} q(\eta,\tau) &= \tau - e^{-\frac{Re}{2}\eta}\left[\tau \cdot \frac{\sinh(\alpha + i\ \beta)\ \ (1-\eta)}{\sinh(\alpha + i\ \beta)} - 2\ \sum_{n=1}^{\infty} \frac{e^{s_1\tau}}{s_1^2} \cdot n\pi\ \sin n\pi\eta\right. \\ &+ \left. \frac{\sinh(\alpha + i\ \beta)\ \eta}{2\ (\alpha + i\ \beta)\sinh^2(\alpha + i\ \beta)} - \frac{\eta\cosh(\alpha + i\ \beta)\ (1-\eta)}{2\ (\alpha + i\ \beta)\sinh(\alpha + i\ \beta)}\right], \end{aligned} \tag{7.26}$$

where α, β and s_1 are given by (7.25).

Equation (7.26) represents the general solution for the unsteady, uniformly accelerated, hydromagnetic flow through a channel with the magnetic lines fixed relative to the fluid.

7.3 Results and discussion

In order to get a physical insight into the problem, a parametric study is performed and the obtained numerical results are elucidated with the help of graphical illustrations. We present the non-dimensional fluid velocity components u_1 and w_1 for several values of the squared-Hartmann number M^2, Hall parameter m, Reynolds number Re and time τ in Figs.7.2-7.6. As $M^2 > 1$, the hydromagnetic drag force is greater than the viscous hydrodynamic force. The case $M^2 = 0$ corresponds to the absence of the applied magnetic field in the fluid flow, the case $m \to \infty$, to the hydrodynamic flow and the case $m = 0$, to the MHD flow in the absence of the Hall currents.

7.3.1 Parameter effects on the primary and secondary velocity profiles

Figs.7.2(a) and 7.2(b) show the time evolution of the primary velocity profile u_1 and secondary velocity profile w_1 at fixed parameters. The primary velocity increases from the zero value at the lower fixed plate to a maximum value at the upper moving plate. The secondary velocity is maximum near the central region of the channel.

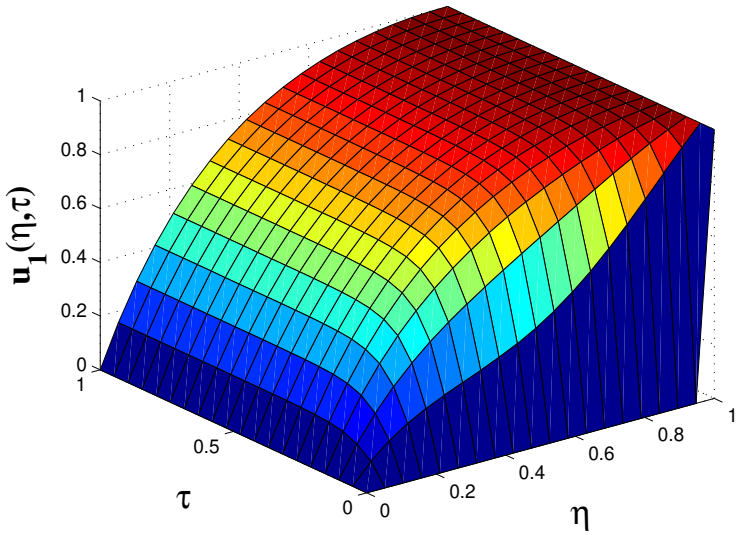

Fig.7.2(a): *Primary velocity profiles across the channel with increasing time when* $M^2 = 10$, $m = 0.2$ *and* $\mathrm{Re} = 0.5$

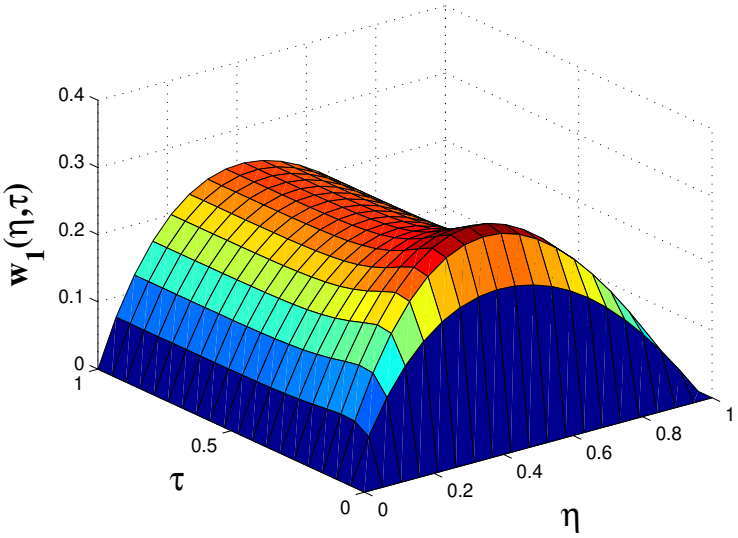

Fig.7.2(b): *Secondary velocity profiles across the channel with increasing time when* $M^2 = 10$, $m = 0.2$ *and* $\mathrm{Re} = 0.5$

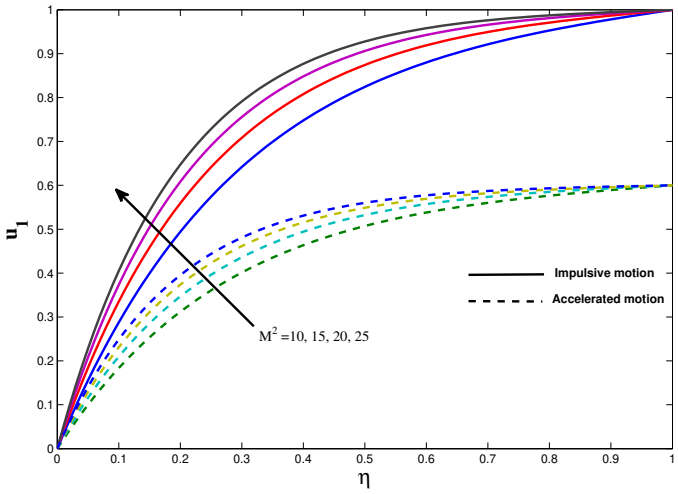

Fig.7.3(a): *Primary velocity for different* M^2 *when* $\mathrm{Re} = 0.5$, $m = 0.2$ *and* $\tau = 0.6$

It is seen from Fig.7.3(a) and 7.3(b) that the primary velocity u_1 increases and the secondary velocity w_1 first increases near the lower plate and then is retarded with increase in the squared-Hartmann number M^2. When a conducting fluid flow is exposed to a magnetic field, the coupling between the flow field and magnetic field occurs. From the physical point of view, it is known that the lines of force representing an applied magnetic field influence the fluid flow. The fluid which is decelerated by the viscous force, receives a push from the magnetic field which counteracts the viscous effects.

Hence, the fluid velocity components increase with M^2.

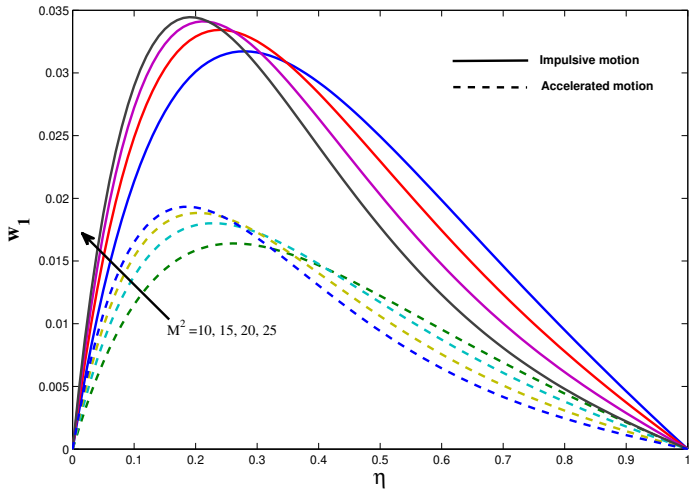

Fig.7.3(b): *Secondary velocity for different* M^2 *when* Re $= 0.5$, $m = 0.2$ *and* $\tau = 0.6$

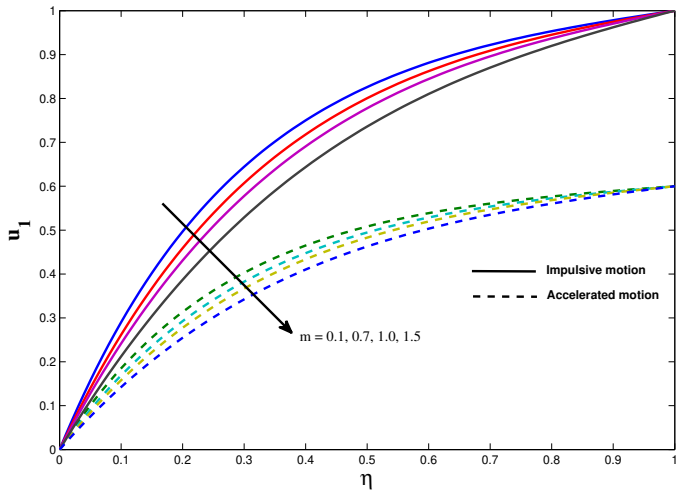

Fig.7.4(a): *Primary velocity for different* m *when* Re $= 0.5$, $M^2 = 10$ *and* $\tau = 0.6$

The primary velocity u_1 decreases with increase in the Hall parameter m, as seen in Fig.7.4(a). The influence of the Hall currents on the secondary fluid velocity w_1 is shown in Fig.7.4(b). It is seen that w_1 increases with m. This is because the effective term $1/(1+m^2)$ decreases as m increases and hence, the resistive effect of the magnetic field is diminished. Since the magnetic field is strong, the electromagnetic force becomes very large, which results in the occurrence of the Hall currents. The secondary velocity is totally dependent on the Hall currents; therefore it can be manipulated by

changing the Hall parameter.

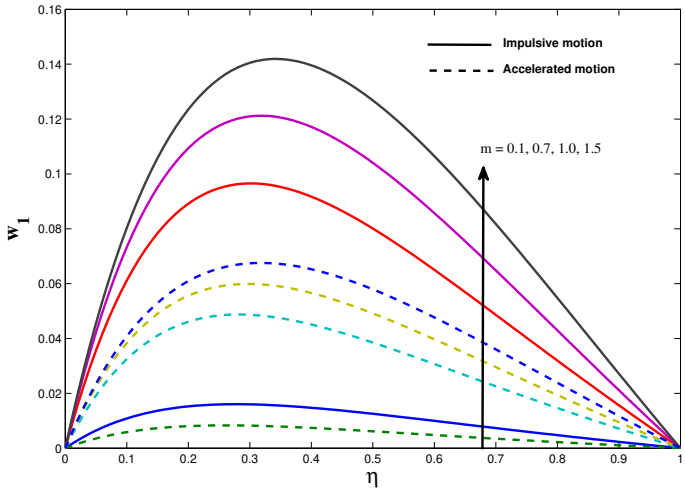

Fig.7.4(b): *Secondary velocity for different* m *when* $\mathrm{Re} = 0.5$, $M^2 = 10$ *and* $\tau = 0.6$

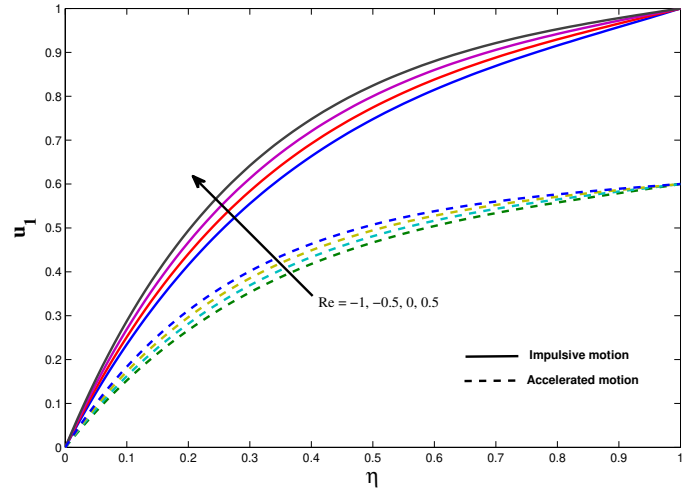

Fig.7.5(a): *Primary velocity for different* Re *when* $M^2 = 10$, $m = 0.2$ *and* $\tau = 0.6$

Figs.7.5(a) and 7.5(b) show that the primary velocity u_1 increases whenever the secondary velocity w_1 decreases with increase in the Reynolds number Re.

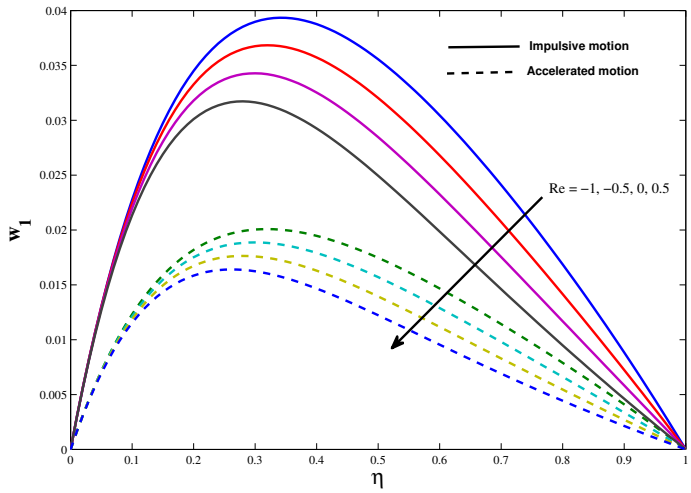

Fig.7.5(b): *Secondary velocity for different* Re *when* $M^2 = 10$, $m = 0.2$ *and* $\tau = 0.6$

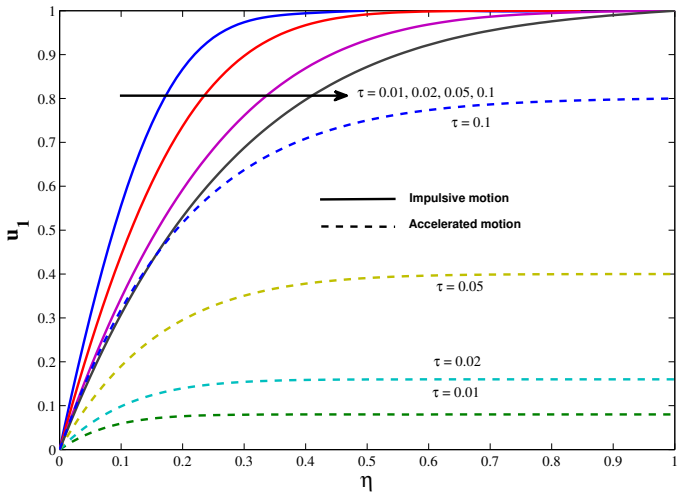

Fig.7.6(a): *Primary velocity for different* τ *when* Re $= 0.5$, $m = 0.2$ *and* $M^2 = 10$

Figs.7.6(a) and 7.6(b) show that the primary velocity u_1 decreases while the secondary velocity w_1 increases with time τ. The velocity components are larger for impulsive motion compared to the uniform acceleration of the upper moving plate, as shown in Figs.7.3-7.6.

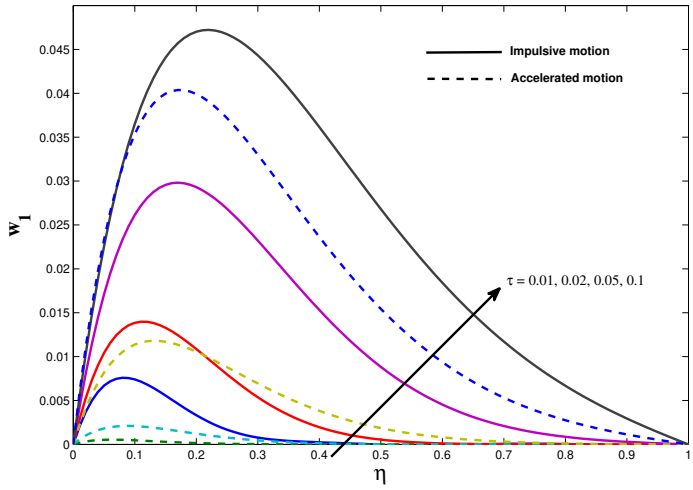

Fig.7.6(b): *Secondary velocity for different* τ *when* $\mathrm{Re} = 0.5$, $m = 0.2$ *and* $M^2 = 10$

7.3.2 Parameter effects on the shear stresses

For engineering design, the shear stresses at the channel plates are important. For impulsive motion, the non-dimensional shear stresses τ_{x_0} and τ_{z_0} at the plate $\eta = 0$ due to the primary and secondary flows are given by

$$\begin{aligned} \tau_{x_0} + i\tau_{z_0} &= \left.\frac{\partial q}{\partial \eta}\right]_{\eta=0} \\ &= \frac{\mathrm{Re}}{2} + (\alpha + i\ \beta)\coth(\alpha + i\ \beta) - 2\sum_{n=1}^{\infty}\frac{e^{s_1\tau}}{s_1}\, n^2\pi^2. \end{aligned} \tag{7.27}$$

For accelerated motion, the shear stresses at the plate $\eta = 0$ are given as

$$\begin{aligned} \tau_{x_0} + i\tau_{z_0} &= \left.\frac{\partial q}{\partial \eta}\right]_{\eta=0} \\ &= \tau\cdot\frac{\mathrm{Re}}{2} + \left[\frac{\tau(\alpha + i\ \beta)\cosh(\alpha + i\ \beta)}{\sinh(\alpha + i\ \beta)}\right. \\ &- \left.\frac{(\alpha + i\ \beta) - \sinh(\alpha + i\ \beta)\cosh(\alpha + i\ \beta)}{2(\alpha + i\ \beta)\sinh^2(\alpha + i\ \beta)}\right] \\ &- 2\sum_{n=1}^{\infty}\frac{e^{s_1\tau}}{s_1^2}\, n^2\pi^2, \end{aligned} \tag{7.28}$$

where α, β and s_1 are given by (7.25).

On separating these equations into real and imaginary parts, one can easily obtain the shear stress components due to the primary and secondary flows for impulsive and accelerated motions.
For impulsive motion, the non-dimensional shear stresses τ_{x_1} and τ_{z_1} at the plate $\eta = 1$ due to the primary and secondary flows are given by

$$\begin{aligned}\tau_{x_1} + i\tau_{z_1} &= \frac{\partial q}{\partial \eta}\Big]_{\eta=1} \\ &= e^{-\frac{\mathrm{Re}}{2}}\left[\frac{(\alpha + i\ \beta)}{\sinh(\alpha + i\ \beta)} - 2\sum_{n=1}^{\infty}(-1)^n \frac{e^{s_1\tau}}{s_1}\, n^2\pi^2\right]. \end{aligned} \tag{7.29}$$

For accelerated motion, the shear stresses at the plate $\eta = 1$ are given as

$$\begin{aligned}\tau_{x_1} + i\tau_{z_1} &= \frac{\partial q}{\partial \eta}\Big]_{\eta=1} \\ &= e^{-\frac{\mathrm{Re}}{2}}\left[\tau\frac{(\alpha + i\ \beta)}{\sinh(\alpha + i\ \beta)} - \frac{(\alpha + i\ \beta)\cosh(\alpha + i\ \beta) - \sinh(\alpha + i\ \beta)}{2(\alpha + i\ \beta)\sinh^2(\alpha + i\ \beta)}\right. \\ &- \left. 2\sum_{n=1}^{\infty}(-1)^n \frac{e^{s_1\tau}}{s_1^2}\, n^2\pi^2\right], \end{aligned} \tag{7.30}$$

where α, β and s_1 are given by (7.25).

The numerical values of the non-dimensional shear stresses at the plate $\eta = 1$ are presented in Figs.7.7 and 7.8 for several values of M^2, m and Re. Figs.7.7(a) and 7.7(b) show that both the shear stresses are reduced when M^2 increases for both kinds of motion of the upper plate. On the other hand, both the shear stresses are enhanced with the Hall parameter m.

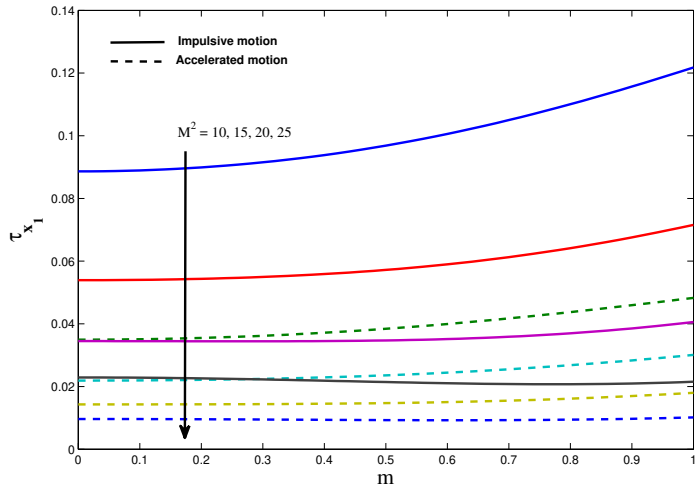

Fig.7.7(a): *Shear stress* τ_{x_1} *for different* M^2 *when* $\mathrm{Re} = 2$ *and* $\tau = 0.5$

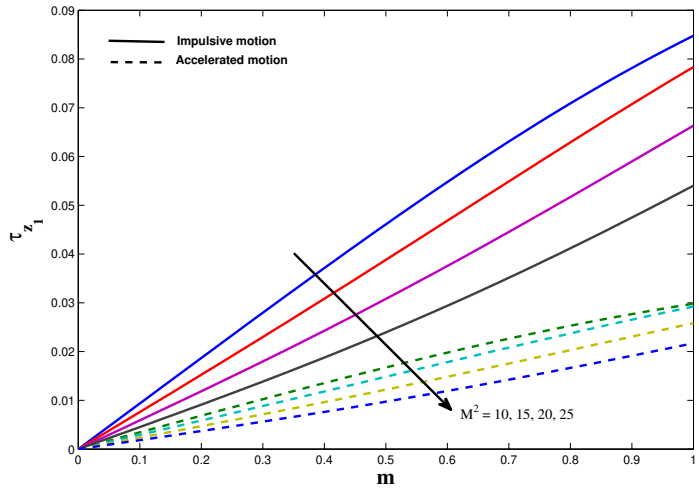

Fig.7.7(b): *Shear stress* τ_{z_1} *for different* M^2 *when* $\mathrm{Re} = 2$ *and* $\tau = 0.5$

An increase in the suction/injection Reynolds number Re leads to a reduction in both the shear stresses τ_{x_1} and τ_{z_1} for both kinds of motion, as shown in Figs.7.8(a) and 7.8(b). The positive values of the shear stresses signify that the moving upper plate exerts a drag force on the fluid along the flow direction.

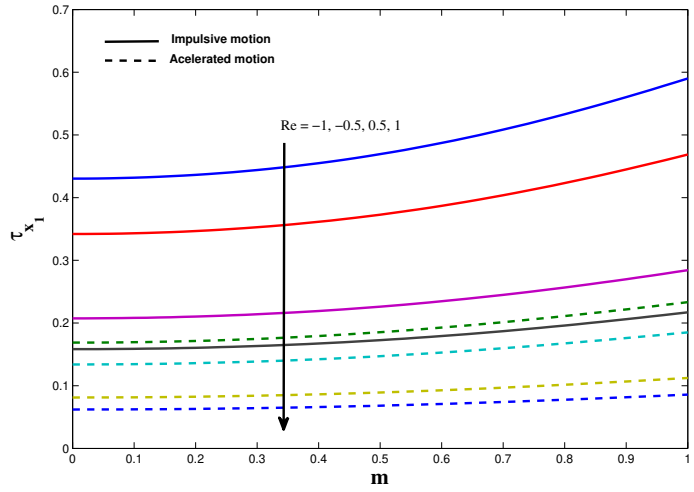

Fig.7.8(a): *Shear stress* τ_{x_1} *for different* Re *when* $M^2 = 10$ *and* $\tau = 0.5$

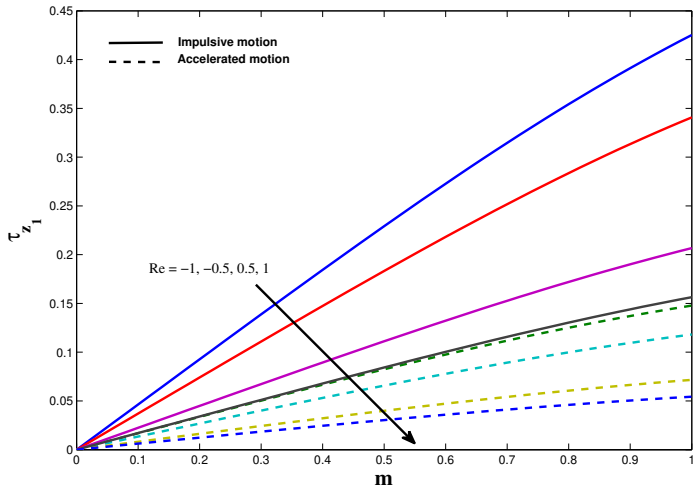

Fig.7.8(b): *Shear stress* τ_{z_1} *for different* Re *when* $M^2 = 10$ *and* $\tau = 0.5$

7.3.3 Heat Transfer

The energy equation taking viscous and Joule dissipations into account is given by

$$\rho c_p \left(\frac{\partial T}{\partial t} - v_0 \frac{\partial T}{\partial y}\right) = \frac{\partial}{\partial y}\left(k\frac{\partial T}{\partial y}\right) + QC_0A_0 \exp\left(-\frac{E}{RT}\right) + \mu\left[\left(\frac{\partial u}{\partial y}\right)^2 + \left(\frac{\partial w}{\partial y}\right)^2\right] + \frac{\sigma B_0^2}{1+m^2}\left[(u-\mathrm{U})^2 + w^2\right], \quad (7.31)$$

where k is the thermal conductivity, c_p the specific heat at constant pressure, T the temperature of the fluid, μ the coefficient of viscosity, Q the heat of reaction, C_0 the initial concentration of reacting species, A_0 the rate constant, R the universal gas constant, E the reaction activity energy. The first term on the right-hand side describes heat conduction, the second term, the Arrhenius reaction, the third term, viscous dissipation and the fourth term, the Joule heating.
The initial and boundary conditions for the temperature are

$$\begin{aligned} &t \leq 0: \;\; T = 0 \;\text{ for }\; 0 \leq y \leq h, \\ &t > 0: \;\; T = T_0 \;\text{ at }\; y = 0 \;\text{ and }\; T = T_0 \;\text{ at }\; y = h. \end{aligned} \tag{7.32}$$

Following [272], the fluid thermal conductivity is assumed to vary exponentially with the temperature as

$$k(T) = k_0 \;\exp\left(m_0(T - T_0)\right) \approx k_0[1 + m_0(T - T_0)], \tag{7.33}$$

where parameter m_0 may be positive for some fluids such as air or water vapour and negative for others like benzene.

Introducing the non-dimensional variable $\theta = \frac{E(T-T_0)}{RT_0^2}$ and using (7.14), equation (7.31) becomes

$$\begin{aligned} \mathrm{Pr}\left(\frac{\partial\theta}{\partial\tau} - \mathrm{Re}\frac{\partial\theta}{\partial\eta}\right) &= \frac{\partial}{\partial\eta}\left[(1+\delta\,\theta)\frac{\partial\theta}{\partial\eta}\right] + \lambda\,\exp\left(\frac{\theta}{1+\epsilon\,\theta}\right) + \mathrm{Pr}\,\mathrm{Ec} \\ &\times\left[\left\{\left(\frac{\partial u_1}{\partial\eta}\right)^2 + \left(\frac{\partial w_1}{\partial\eta}\right)^2\right\} + \frac{M^2}{1+m^2}\left\{(u_1 - f(\tau))^2 + w_1^2\right\}\right], \end{aligned} \tag{7.34}$$

where $\lambda = \frac{QA_0C_0E\,h^2}{RT_0^2k_0}\,\exp\left(-\frac{E}{RT_0}\right)$ is the Frank-Kamenetskii parameter or the reaction rate parameter, $\epsilon = \frac{RT_0}{E}$ the activation energy parameter, $\delta = \frac{m_0\,R\,T_0^2}{E}$ the thermal conductivity variation parameter, $\mathrm{Pr} = \frac{\rho\,\nu\,c_p}{k_0}$ the Prandtl number which is defined as the ratio of the momentum diffusivity (kinematic viscosity) to the thermal diffusivity and $\mathrm{Ec} = \frac{E\,u_0^2}{c_pRT_0^2}$ the Eckert number which expresses the relationship between the kinetic energy and flow enthalpy. The Eckert number is used in high altitude rocket aero-thermodynamics.
The corresponding initial and boundary conditions are

$$\begin{aligned} &\theta(\eta, 0) = 0 \;\text{ for }\; 0 \leq \eta \leq 1, \\ &\theta(0, \tau) = 0 \;\text{ and }\; \theta(1, \tau) = 0 \;\text{ for }\; \tau > 0. \end{aligned} \tag{7.35}$$

The analytical solutions for the fluid velocity given by equations (7.24) and (7.26) are used in equation (7.34) and the resulting differential equation with boundary conditions (7.35) is solved numerically with the help of MATLAB software package. For the analysis of the heat transfer characteristics in the flow, the energy equation is taken where all the convective terms equal to zero because of the assumed temperature boundary conditions. Therefore, the temperature distribution in the channel is due to the heat generation by the viscous and Joule dissipations and conduction through the fluid in the transverse direction. The Prandtl number (Pr) is chosen as $0.72 \leq \mathrm{Pr} \leq 2$, since such values of Pr are typical of most of the fluids used in plasma physics, engineering and industries. The case $\mathrm{Ec} = 0$ represents the absence of viscous and Joule heating.

7.3.4 Parameter effects on the temperature profiles

Fig.7.9 shows the time evolution of the reactive fluid temperature profiles across the channel for the fixed set of parameters. The temperature first decreases, reaches a minimum in the central region of the channel and then increases.

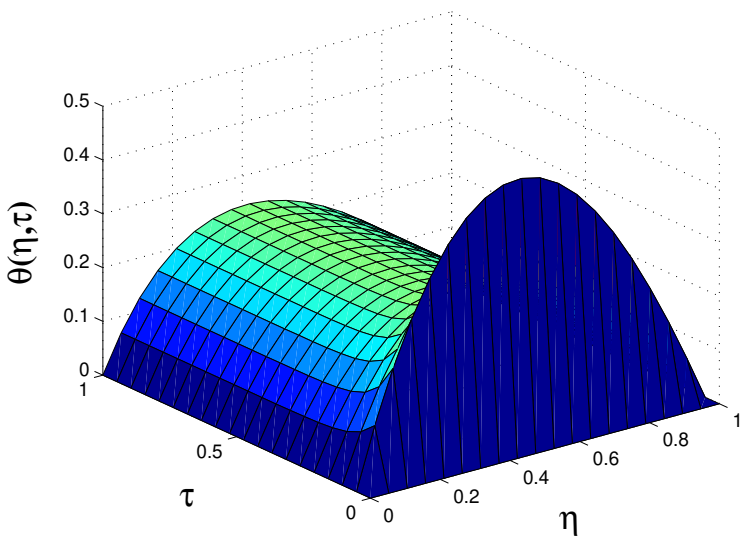

Fig.7.9: *Temperature profiles across the channel with increasing time when* $M^2 = 5$, $m = 0.1$, $\mathrm{Re} = 1$, $\mathrm{Pr} = 0.72$, $\mathrm{Ec} = 0.1$, $\delta = 0.1$, $\lambda = 0.1$ *and* $\varepsilon = 0.1$

Fig.7.10 shows that the fluid temperature θ rises with the squared-Hartmann num-

ber M^2 for both kinds of motion of the upper plate. This may be explained as the effect of the internal heating generation due to the Joule dissipation.

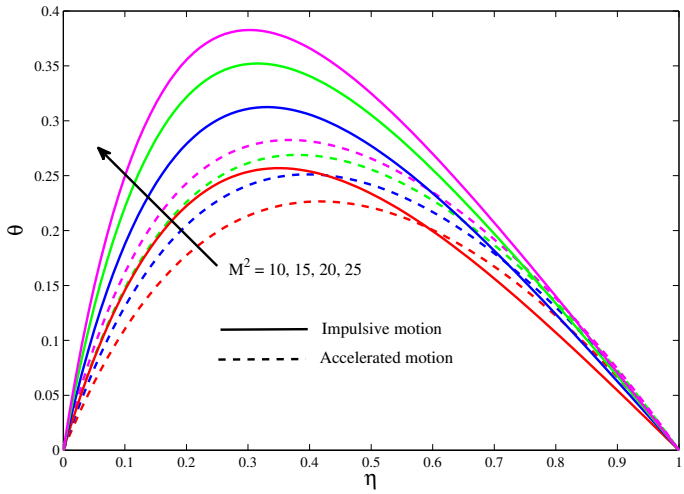

Fig.7.10: *Temperature profiles for different* M^2 *when* $\mathrm{Re} = 1$, $\mathrm{Pr} = 0.72$, $m = 0.1$, $\mathrm{Ec} = 0.1$, $\lambda = 0.1$, $\delta = 0.1$, $\tau = 0.1$ *and* $\varepsilon = 0.1$

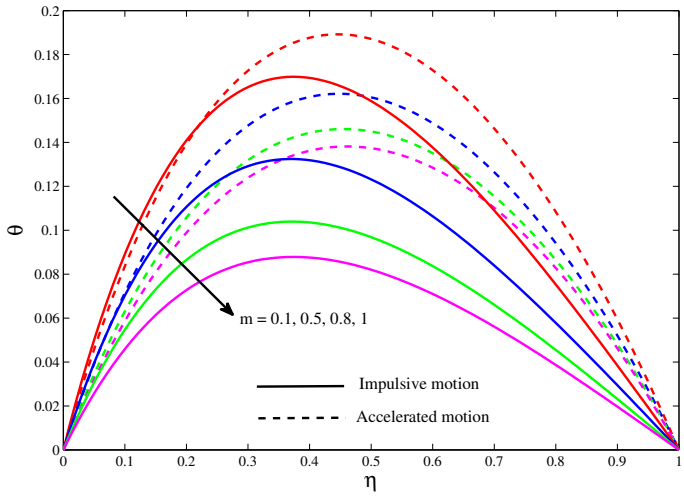

Fig.7.11: *Temperature profiles for different* m *when* $M^2 = 5$, $\mathrm{Pr} = 0.72$, $\mathrm{Re} = 1$, $\mathrm{Ec} = 0.1$, $\delta = 0.1$, $\lambda = 0.1$, $\tau = 0.1$ *and* $\varepsilon = 0.1$

Fig.7.11 reveals that the fluid temperature θ decreases with increase in the Hall parameter m. Fig.7.12 shows that the fluid temperature θ increases with the suction/injection parameter Re. This is because the reactive fluid is sucked from the channel.

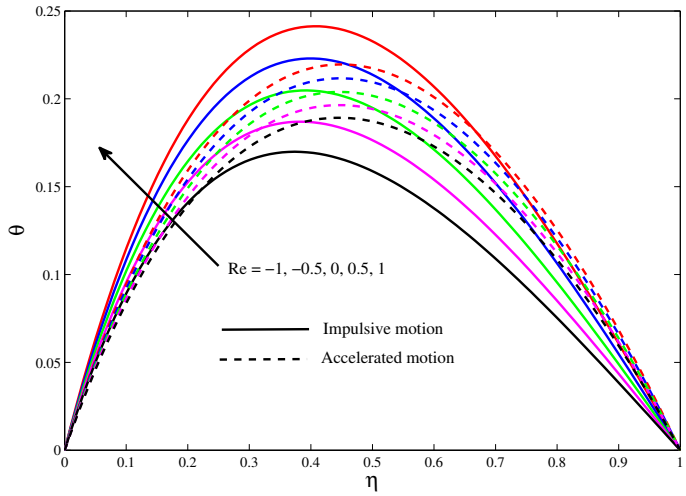

Fig.7.12: *Temperature profiles for different* Re *when* $M^2 = 5$, Pr $= 0.72$, $m = 0.1$, Ec $= 0.1$, $\lambda = 0.1$, $\delta = 0.1$, $\tau = 0.1$ *and* $\varepsilon = 0.1$

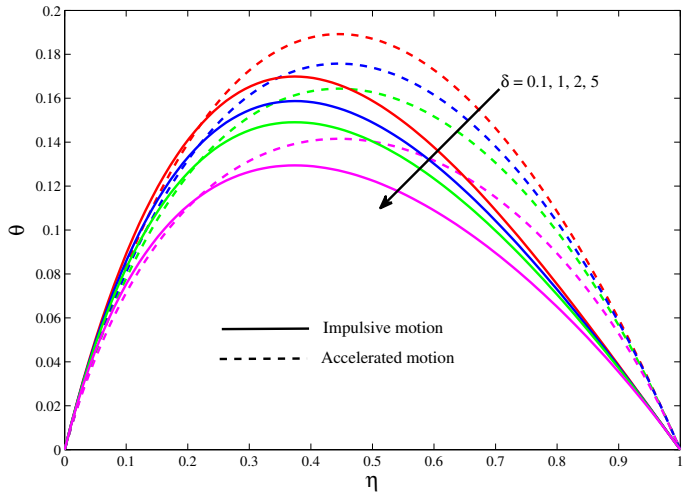

Fig.7.13: *Temperature profiles for different* δ *when* $M^2 = 5$, Pr $= 0.72$, $m = 0.1$, Ec $= 0.1$, Re $= 1$, $\lambda = 0.1$, $\tau = 0.1$ *and* $\varepsilon = 0.1$

Fig.7.13 shows that θ decreases with increase in the variable conductivity parameter δ. As δ increases, the viscous heating effect decreases.

7.3.5 Parameter effects on the rate of heat transfer

The numerical results for the rate of heat transfer $-\theta'(1,\tau)$ at the upper plate $\eta = 1$ for several values of the suction/injection Reynolds number Re and the thermal con-

ductivity variation parameter δ are presented in Figs.7.14 and 7.15. These figures show that $-\theta'(1,\tau)$ decreases with increase in either Re or δ for both cases of motion. As δ increases, the thermal conductivity of the fluid is enhanced and hence, heat can diffuse from the moving plate faster. As a result, the rate of heat transfer at the moving plate decreases.

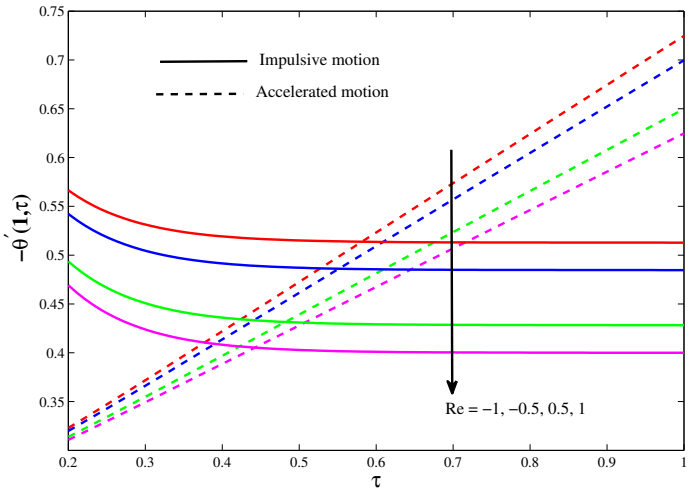

Fig.7.14: *Rate of heat transfer* $\theta'(1,\tau)$ *for different* Re *when* Ec $= 0.1$, $m = 0.1$, Pr $= 0.72$, $M^2 = 5$, $\delta = 0.1$, $\lambda = 0.1$ *and* $\varepsilon = 0.1$

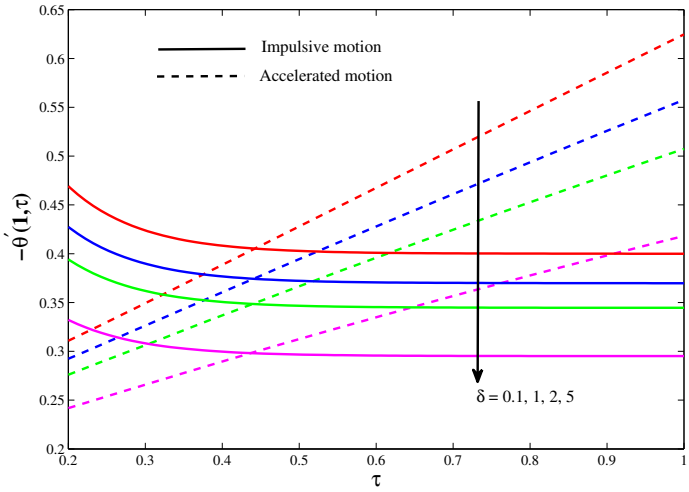

Fig.7.15: *Rate of heat transfer* $\theta'(1,\tau)$ *for different* δ *when* Re $= 1$, $m = 0.1$, Pr $= 0.72$, $M^2 = 5$, Ec $= 0.1$, $\lambda = 0.1$ *and* $\varepsilon = 0.1$

7.4 Conclusion

We have examined the influences of Hall currents on an unsteady hydromagnetic flow and heat transfer of a reactive viscous incompressible electrically conducting fluid between two infinitely long horizontal parallel porous plates in the presence of a uniform transverse magnetic field when one of the plate is set into impulsive/uniformly accelerated motion under the Arrhenius reaction rate. The unified analytical expressions for the velocity field and shear stresses have been derived in a closed form, using the Laplace transform technique. The energy equation is solved numerically, using Matlab. Based on the graphical presentations, the following conclusions can be summarized:

- The velocity of a reactive viscous fluid in the channel is significantly modified by the combined effects of the magnetic field and Hall currents.
- The primary velocity is enhanced while the secondary velocity decreases due to uniform suction/injection.
- The secondary velocity of a reactive viscous fluid increases with time.
- The temperature of the reactive viscous fluid in the channel is reduced with increase in the Hall parameter or the variable thermal conductivity parameter, while it increases with the squared-Hartmann number or suction/injection parameter.
- The shear stresses at the channel plates increase with Hall currents while they are reduced with increasing squared-Hartmann number or suction/injection parameter.
- The rate of heat transfer at the channel plates is reduced due to increase in either variable thermal conductivity parameter or suction/injection parameter.